Wall-Interference Corrections for Parachutes in a Closed Wind Tunnel

J. Michael Macha* and Robert J. Buffington†
Sandia National Laboratories, Albuquerque, New Mexico 87185

A set of 6-ft-diam ribbon parachutes (geometric porosities of 7, 15, and 30%) was tested in various subsonic wind tunnels covering a range of geometric blockages from 2 to 35%. Drag, base pressure, and inflated geometry were measured under full-open, steady-flow conditions. The resulting drag areas and pressure coefficients were correlated with the bluff-body blockage parameter (i.e., drag area divided by tunnel cross-sectional area) according to the blockage theory of Maskell. The data show that the Maskell theory provides a simple, accurate correction for the effective increase in dynamic pressure caused by wall constraint for both single parachutes and clusters. For single parachutes, the empirically derived blockage factor K_M has the value of 1.85, independent of canopy porosity. Derived values of K_M for two- and three-parachute clusters are 1.35 and 1.59, respectively. Based on the photometric data, there was no deformation of the inflated shape of the single parachutes up to a geometric blockage of 22%. In the case of the three-parachute cluster, decreases in both the inflated diameter and the spacing among member parachutes were observed at a geometric blockage of 35%.

Nomenclature

C	= tunnel cross-sectional area
C_DS	= model drag area, D/q
C_p	= pressure coefficient, $(p - p_s)/q$
D	= model drag force
D_c	= canopy constructed diameter, 6 ft approx.
K_M	= Maskell bluff-body blockage factor
L_r	= riser length
L_s	= suspension line length, 6 ft
N	= number of parachutes in a cluster
p	= canopy surface pressure
p_s	= freestream static pressure
q	= freestream dynamic pressure

Subscript

u	= uncorrected for wall interference

Introduction

BECAUSE of the complexity of the fluid dynamics involved, advances in parachute technology rely heavily on experimentation. The wind tunnel offers an attractive alternative to flight testing especially when the objective of the investigation is independent of the large decelerations many systems undergo. As always, aerodynamic measurements made in a wind tunnel are subject to errors caused by the flow-constraining influence of the tunnel walls. Prudent testing practice dictates that the size of the model relative to that of the tunnel be consistent with the ability to correct for this effect. In the case of parachutes, there is no generally accepted procedure for treating wall interference; individual investigators apply corrections on an ad hoc basis, often using adaptations of methods developed for models other than parachutes.

The applicability of the various correction methods and the accuracy of the reported data should be viewed with some skepticism because of the unique features of a parachute compared to other aerodynamic devices. For example, the large wake emanating from the canopy causes the interference to be greater for a parachute than for a streamlined body with the same frontal area and thus precludes the use of simple methods based on potential theory. In addition, the inflated shape of a parachute will be distorted if the wall constraint is severe enough. And in the case of multiple-parachute clusters, the measured performance may be further in error due to a change in the spacing among members of the cluster. Finally, the relatively large dimensional tolerances associated with fabric construction and the requirement to replicate material elastic properties place a practical limit on the miniaturization of parachutes. This restriction on model scale often makes it difficult to observe even a modest upper limit on geometric blockage (i.e., the ratio of model frontal area to tunnel area), except in the few largest wind tunnels in existence.

The purpose of this investigation was to generate an adequate experimental data base for single parachutes and multiple-parachute clusters with which to formulate and validate an accurate correction method. The models used were of ribbon design covering a range of geometric porosities, but the results are believed to be applicable to any parachute of circular or conical construction. Use of the correction method should significantly increase confidence in future wind tunnel data and may stimulate a more extensive use of wind tunnels by increasing the acceptable upper limit on geometric blockage.

Theory of Wall Corrections

In a solid-wall test section, the blocking effect of the wall on the free displacement of streamlines causes velocities in the vicinity of a model to increase. If the resulting extraneous pressure gradient over the length of the model is not too great, the character of the viscous flow (i.e., the boundary layer thickness and locations of flow separation) remains essentially the same as in an unconstrained airstream. Under these conditions, model force and pressure measurements can be adequately corrected on the basis of the average increase in dynamic pressure along the tunnel centerline. That is, in incompressible flow,

$$\frac{C_DS_u}{C_DS} = \frac{(1 - C_{p,u})}{(1 - C_p)} = \frac{q}{q_u} \tag{1}$$

Presented as Paper 89-0900 at the AIAA 10th Aerodynamic Decelerator Systems Conference, Cocoa Beach, FL, April 18-20, 1989; received May 13, 1989.

*Senior Member of Technical Staff, Parachute Systems Division. Senior Member AIAA.

†Senior Member of Technical Staff, Experimental Aerodynamics Division. Member AIAA.

where variables without subscripts are corrected quantities.

The ability to predict the increase in dynamic pressure is directly related to how amenable the flow around the body is to mathematical description. For streamlined shapes, the interference velocity field is readily determined from a representation of the walls, the body, and the narrow-trailing wake with potential flow singularities. The computational part of this approach has been reduced to a chart look-up procedure as presented in Ref. 1.

In the case of a bluff body such as a parachute, the large wake dominates the flowfield and the wall-constraint problem. The internal mechanics of the wake are not well enough understood to be modeled accurately by singularities without additional flowfield measurements such as the static pressure distribution along the tunnel wall. The evolution of this "pressure signature" method has been documented by Hackett,[2] and there is no reason to doubt its applicability to parachutes. However, the pressure signature method requires tunnel instrumentation and on-line computing resources that are not yet in place at most wind tunnels. In the interim, there exists a need for an approximate, explicit correction procedure of acceptable and verified accuracy. Quantitative information on the deformation of individual parachutes and parachute clusters at high blockages is also needed, since a change in model geometry makes any attempt at wall correction a dubious undertaking.

An approximate correction method of proven accuracy for a variety of nonlifting two- and three-dimensional bluff bodies has been developed by Maskell.[3] This method is based on an approximate form of the momentum equation applied to the control volume bounded by the tunnel walls, the body, and a constant pressure surface defining the near wake. Two additional empirically derived relations match the behavior of the model under wall constraint to observation. One of the auxiliary equations follows from the assumption that the geometric blockage is not so great that the proximity of the tunnel wall alters the form of the pressure distribution about the model. This assumption is essentially satisfied if there is no displacement of the flow-separation line and, in the case of a flexible model, no deformation. The second auxiliary relation accounts for the distortion of the wake under constraint. The form of this relation was derived from test results for square plates but is supposed to hold generally for bluff bodies in incompressible flow.

According to Maskell, the effective increase in dynamic pressure is given by

$$\frac{q}{q_u} = 1 + K_M \frac{C_D S_u}{C} \tag{2}$$

Since K_M is independent of the degree of wall constraint, and the geometric blockage does not appear explicitly, Eq. (2) is especially suited to on-line correction during data acquisition for parachutes where the inflated shape may not be known a priori.

According to additional details of Maskell's theory,[3] K_M is equal to the negative reciprocal of the average base pressure coefficient in an unconstrained flow. That is,

$$K_M = -\frac{1}{C_{p,b}} \tag{3}$$

For the body shapes originally considered by Maskell (i.e., thin, square plates normal to the flow), the near wake is a region of nearly constant pressure. In this case, Eqs. (1-3) can be used to determine K_M from measurements of $C_D S_u$ and a single pressure somewhere on the base of the model.

For bluff shapes with appreciable depth in the flow direction, Eq. (2) is still valid but the relationship between K_M and the average base pressure may require modification. In a study of two-dimensional rectangular prisms, Awbi[4] found it was necessary to include a multiplicative factor Λ on the right side of Eq. (3). As the depth-to-height ratio of the prism increased from near zero (i.e., a thin plate), Λ first increased to values >1 and then monotonically decreased to values <1.

For some bluff bodies, including parachutes, pressure is not uniform over the base, and the average value must be determined from a survey of the surface. In practice, other constraints on model design often prevent the incorporation of a sufficient number of measurement orifices.

In any event, K_M can be evaluated for a particular body or family of similar bodies by directly fitting Eqs. (1) and (2) to pressure or drag measurements made on models over a range of geometric blockages. This approach has been used previously by Pass[5] for triangular plates and by Awbi and Tan[6] for spheres.

The unique feature of a parachute compared to other bluff bodies is its flexibility and the fact that the inflated shape is determined by a state of equilibrium between internal stresses and surface pressures. To maintain a constant geometry in any experimental wall-effects study, it is necessary to keep constant the ratio of corrected dynamic pressure to the effective elastic modulus of the model. At geometric blockages below which model distortion occurs, the blockage factor K_M for an individual parachute should then depend on the physical characteristics which influence the inflated shape; these may include canopy type (solid, ribbon, guide surface, cruciform, etc.) and the stage of inflation (i.e., full open or reefed). The value of K_M for a cluster of parachutes should depend on the collective shape presented to the airstream, which may be influenced by the length of risers used as well as canopy type.

Experimental Program

General Procedure

The experimental procedure consisted of measuring drag, base pressure, and airstream properties for a set of nonreefed parachutes in wind tunnels of different sizes. Compared to the alternate approach of testing different size but geometrically similar parachutes in a single wind tunnel, the procedure used has the advantage of eliminating extraneous scale effects that might obscure the true wall-interference effects. Specifically, the difficulty during model fabrication of maintaining precise geometric similarity among canopies of different diameters was avoided. Furthermore, by testing a one-size parachute at a set drag level, the corrected airstream velocity is necessarily constant regardless of the tunnel size. Then, the dynamic similarity parameters, which are functions of velocity and which determine the aerodynamic performance and inflated geometry of the parachute (i.e., Mach and Reynolds numbers and the elasticity parameters), are duplicated as well.

The variable among the set of models was geometric porosity. Single parachutes were tested in each wind tunnel at a fixed drag level of 250 lb, or equivalently, at corrected dynamic pressures of 13-19 psf depending on their porosity. The same method was used for the clusters of two and three parachutes with the drag set at 500 and 750 lb, respectively. Movie and still cameras recorded model geometry.

The approximate test-section dimensions of the solid-wall wind tunnels used in the study and the resulting geometric blockage ratios for a single parachute are listed in Table 1. For convenience, specific wind tunnels will be cited by number in the following discussions. Except for tunnel 4, the test

Table 1 Wind tunnels used in the blockage study

Wind tunnel	Geometric blockage
1) Lockheed 30 × 26 ft	0.019
2) NASA Langley 14 × 22 ft	0.048
3) NASA Lewis 9 × 15 ft	0.116
4) General Dynamics 8 × 12 ft	0.166
5) NASA Ames 7 × 10 ft	0.217
6) Vought 7 × 10 ft	0.217

sections were rectangular in cross section; tunnel 4 was rectangular with 45-deg filleted corners. Single-parachute configurations were tested in all six of the wind tunnels, but the clusters of two and three parachutes were tested in tunnels 1–3 only.

Models and Tunnel Installation

The models used in the tests were 6-ft-diam, 12-gore ribbon parachutes with a 20-deg constructed cone angle. Typical model dimensions are shown in Fig. 1. Spacing between the 1-in.-wide ribbons was adjusted to provide a uniform geometric porosity from vent to skirt of 7, 15, or 30%. Canopy materials were nylon tape (MIL-T-5038, Type III) with sufficient strength to limit elastic elongation to less than 1% at the test dynamic pressure. The Kevlar suspension lines (MIL-C-87129, Type IV, 400 lb) were 6-ft long.

A pressure orifice was located on the outside centerline of each gore, 12 in. from the apex. Examination of data reported by Pepper and Reed[7] for parachutes of similar construction had shown that the pressure at this location is approximately equal to the radially averaged pressure. The orifices consisted of 0.035-in.-diam holes drilled in 0.5-in.-diam by 0.125-in.-thick rigid plastic disks firmly sewn to the outer surface of the canopy. The 12 orifices were manifolded together with flexible tubing and connected to a single length of tubing attached to one of the suspension lines.

The same method of model installation was used in each facility and was designed to minimize structure volume and associated flow interference. The parachutes were attached to a single-component load cell mounted inside a 3.2-in.-diam by 18-in.-long ogive-cylinder support body. The support body was suspended on the centerline of the tunnel by four 0.125-in.-diam steel cables. The drag of the system was reacted by a cable or steel rod from the nose of the support body to a yoke and then by a pair of 0.25-in.-diam cables to the tunnel side walls. The plastic tubing from the manifolded pressure orifices was routed across the load cell and down one of the support-body centering cables to a transducer outside the test section. General features of the installation are illustrated in Fig. 2.

For the single parachutes, the actual coupling of the suspension lines to the load cell was through 12 individual attachment points on a circle of 1.25-in. radius. Under load, this scheme produced sufficient torsional resistance to prevent the parachutes from rotating due to slight asymmetries in their construction.

The cluster configurations were composed of two or three of the 15%-porous parachutes. Risers were added between the confluence point of the suspension lines and the load-cell assembly with the length of the risers relative to that of the suspension lines given by the equation

$$\frac{L_r}{L_s} = \sqrt{N} - 1 \tag{4}$$

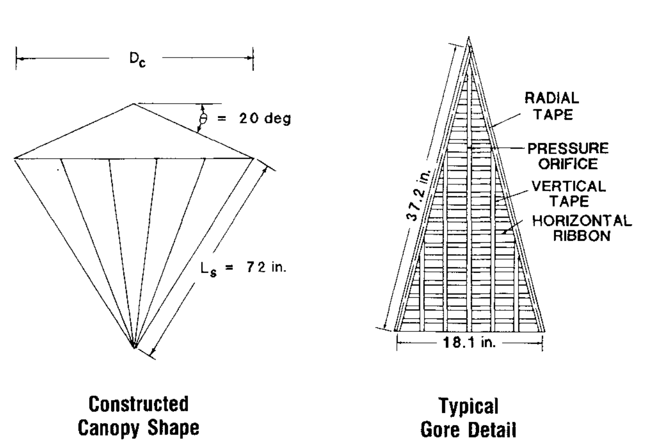

Fig. 1 Parachute dimensional data.

To prevent members of a cluster from rotating about each other, the parachutes were tethered together at the skirt with 2-ft lengths of cord. In the first test of the series (tunnel 2), it was found necessary to attach an additional tether from one of the parachutes to the tunnel floor to prevent rotation of the cluster as a unit. In subsequent tests, a rotary bearing was added to the base of the load-cell assembly to allow the clusters to rotate at will. It should be noted that the clusters did not rotate continuously; occasionally, part of one revolution would occur with a return to a stable geometry. With the addition of the swivel, it was not possible to measure canopy surface pressures for the clusters.

Measurement Uncertainty

The uncorrected dynamic pressure at the model location was measured in terms of the pressure difference between two sets of wall orifices ahead of the test section. Typically, the downstream set was at or near the end of the contraction. If a model is sufficiently large, its presence may affect the static pressure in this region. The resulting error in q_u would obscure the genuine wall-interference effects. A supplemental investigation of the effects of the proximity of the model to the wall orifices was conducted in tunnel no. 6. The results confirmed that the orifices were far enough removed from the models to accurately determine q_u in all of the facilities used.

Based on demonstrated transducer accuracy, the uncertainty in all pressure measurements, including tunnel dynamic pressure, was ± 0.1 psf. The instrument uncertainty in the measurement of model drag was ± 1 lb. The propagation of uncertainties in results calculated from these measurements was estimated using the method of Kline and McClintock (see, e.g., Ref. 8). The maximum uncertainties in the reported data, as a percentage of the quoted values, are as follows: drag area, $\pm 1.5\%$; pressure coefficient, $\pm 4\%$. The inflated diameters of the models, which were determined from photometric data, have an estimated uncertainty of $\pm 1.5\%$.

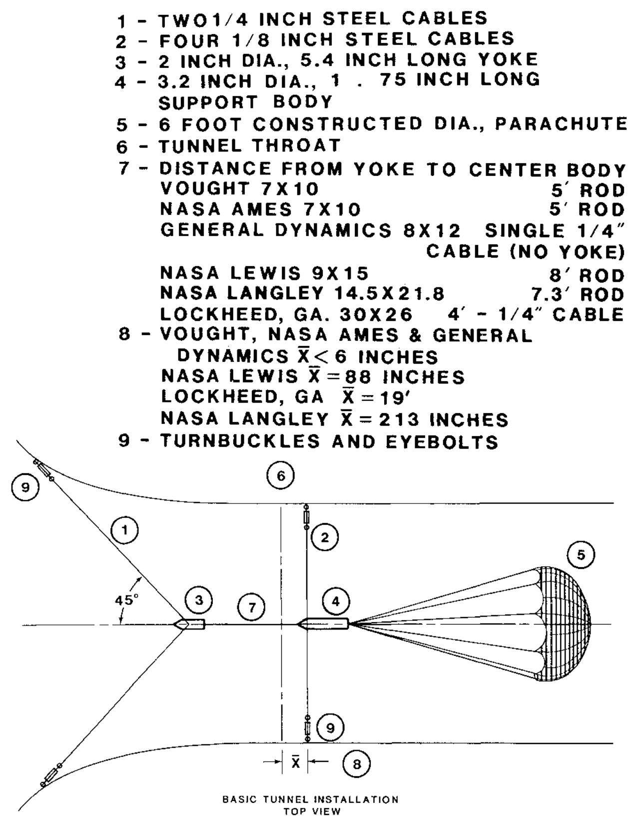

Fig. 2 Wind-tunnel installation details.

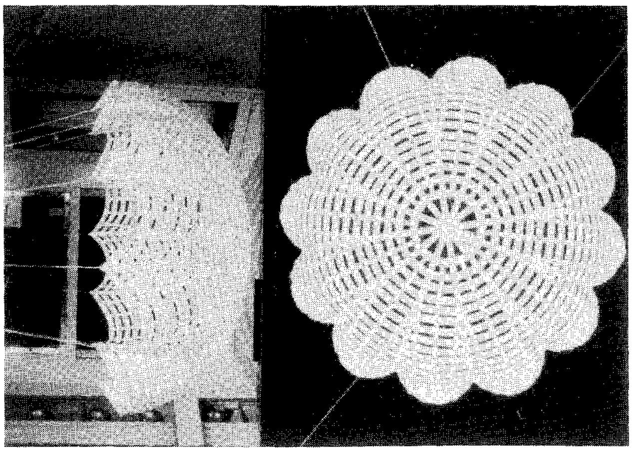

Fig. 3 Inflated shape of the 30%-porous model in tunnel 4.

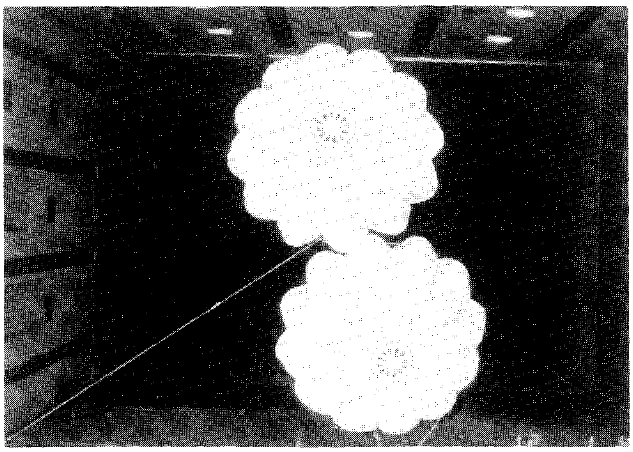

Fig. 4 View from downstream of the two-parachute cluster in tunnel 2.

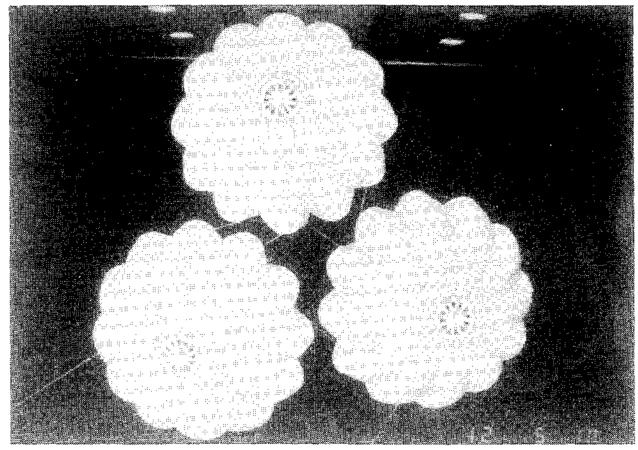

Fig. 5 View from downstream of the three-parachute cluster in tunnel 2.

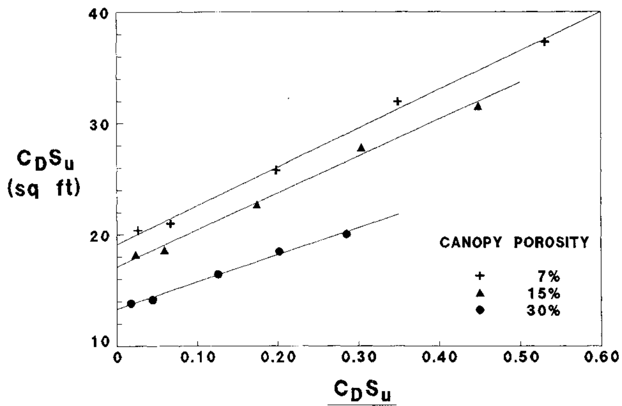

Fig. 6 Variation in single-parachute, uncorrected drag area with the Maskell bluff-body blockage parameter.

The overall quality of the data was enhanced by averaging values over an appropriate time scale, and by obtaining multiple measurements at each blockage from two or three identical parachute models and/or repeated measurements from the same model.

Experimental Results

Model Inflated Geometry

Analysis of the photometric data for the single-parachute configurations showed that there was no change in inflated shape over the range of geometric blockages investigated. The midgore diameters of the 7-, 15-, and 30%-porous models were 54.5, 55.1, and 52.3 in., respectively. Figure 3 illustrates the inflated shape of the 30%-porous model from orthogonal views; the general features shown are typical of the 7- and 15%-porous models as well.

The maximum geometric blockage investigated for the cluster of two 15%-porous parachutes was 0.232 in tunnel no. 3. There was no observable effect of wall constraint on either the inflated shape of a member parachute or the spatial relation between the two parachutes. The canopies remained in contact with each other as shown in Fig. 4, with the risers making an angle of approximately 30 deg.

The greatest geometric blockage for the cluster of three parachutes was 0.348, also in tunnel no. 3. At the lower blockage ratios in tunnels 1 and 2, the cone angle formed by the risers was approximately 29 deg; in tunnel no. 3, the cone angle decreased to approximately 26.5 deg, and the midgore diameter of a member parachute decreased to 53.2 in. This change in geometry represents a 12% decrease in the area of a circle circumscribing the three canopies. Figure 5 shows the geometry of the three-parachute cluster in tunnel no. 2.

Drag Area and Pressure Coefficient

In Fig. 6, the uncorrected drag areas for single parachutes are plotted as a function of the Maskell blockage parameter (i.e., uncorrected drag area divided by the tunnel cross-sectional area). As predicted by Eqs. (1) and (2), the data exhibit a linear dependence within measurement accuracy.

The canopy pressures measured on the single-parachute configurations have been put in coefficient form as shown in Fig. 7. As expected, the uncorrected coefficients also exhibit a linear dependence on the Maskell blockage parameter. The data further show that variation in the pressure coefficient with canopy porosity is within the measurement uncertainty. Drag-area measurements for the cluster configurations are shown in Fig. 8 by the solid symbols. The three data points for the two-parachute cluster clearly establish a linear variation with the Maskell blockage parameter. In the case of the three-parachute cluster, the test results at the largest blockage ratio must be discounted because of the geometry change discussed previously. The open symbols are inferred from the single parachute data and are discussed below.

Method of Wall Correction

Single Parachute

Linear, least-squares approximations were made to the variations of drag area and pressure coefficient with the Maskell blockage parameter as indicated by the solid lines in Figs. 6 and 7. The vertical-axis intercepts represent values corrected

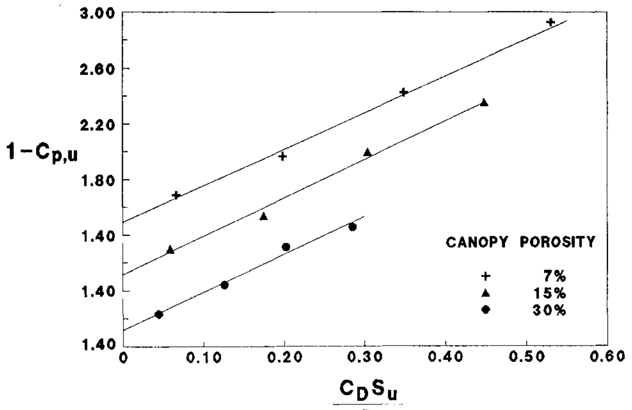

Fig. 7 Variation in uncorrected base-pressure coefficient with the Maskell bluff-body blockage parameter.

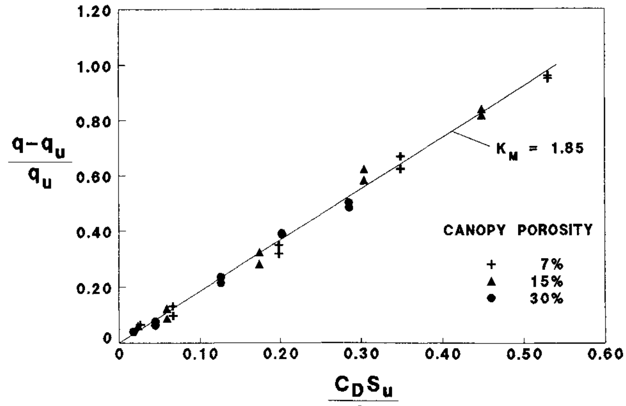

Fig. 9 Correction to dynamic pressure for single parachutes.

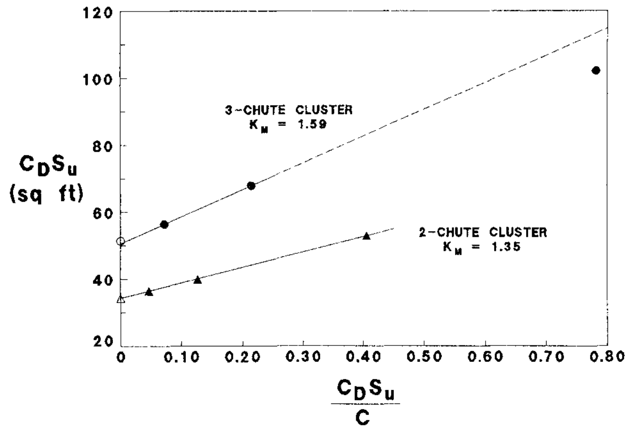

Fig. 8 Variation in cluster uncorrected drag area with the Maskell bluff-body blockage parameter.

for the effects of wall constraint. The corrected drag areas in units of ft^2 are 19.1, 17.1, and 13.3 for canopy porosities of 7, 15 and 30%, respectively. Corresponding corrected pressure coefficients are -0.49, -0.51, and -0.52. As stated earlier, the observed variation in pressure coefficient with canopy porosity is within the measurement uncertainty. Assuming the pressure at the measurement location is representative of the average base pressure, Maskell's theory [i.e., Eq. (3)] gives $K_M \approx 2.0$.

A strictly empirical evaluation of K_M, which makes use of the drag-area measurements as well as the pressure measurements, is achieved by directly fitting Eqs. (1) and (2) to the data. The result of this procedure is shown in Fig. 9. The same type of symbol has been used for both drag area and canopy pressure for a given porosity as indicated by the pair of symbols at each value of the blockage parameter. The data illustrate a high degree of conformity between the independent measurements of drag area and base pressure in determining the effective increase in dynamic pressure. The best-fit value of K_M to the composite data for all three canopy porosities is 1.85. A plausible explanation for the small discrepancy between this value and the 2.0 based on Eq. (3) is a slight difference between the locally measured and average base pressures or possibly the failure to include an appropriate Λ factor as suggested by Awbi.[4]

The derived blockage factor of 1.85 for parachutes compares favorably to those of 2.8 for a nonporous disk (evaluated from data reported in Ref. 9) and of 3.6 for a sphere in subcritical flow.[6] Generally, K_M is greater for shapes with lower drag coefficients. The corrected drag coefficient based on solid frontal area of the inflated canopy (i.e., excluding the fraction of open area between ribbons) was approximately 1.35 for all three porosities. In comparison, typical values of the drag coefficient for a disk and a sphere are 1.18 and 0.46, respectively.

Parachute Clusters

The drag area measurements for the cluster configurations were analyzed in the same manner as those for the single parachutes. The lower set of data in Fig. 8 shows a linear relation between uncorrected drag area and the bluff-body blockage parameter for the two-parachute cluster. The best-fit value of K_M for the three data points represented by the solid triangles is 1.35. Data from the wind tunnel investigation of cluster performance by Baca[10] have been re-examined in light of the present wall-interference results. For riser lengths given by Eq. (4), those data now show that the drag area of a cluster of N parachutes is equal to N times the drag area of a single parachute within an estimated measurement uncertainty of $\pm 3\%$. The frequently observed reduction in drag efficiency as the number of parachutes in a cluster increases occurs only with risers shorter than those used in the present study. The open triangle on the vertical axis of Fig. 8 represents twice the corrected drag area of a single 15%-porous canopy from Fig. 6. The excellent agreement between the single parachute and cluster data is reassuring given the relatively small number of data points for the cluster.

The upper set of data in Fig. 8 is for the three-parachute cluster. The data point at the greatest blockage has been ignored in evaluating the Maskell blockage factor because of the geometry distortion described earlier. For the two remaining data points, $K_M = 1.59$. Again, the excellent agreement between the extrapolation of the cluster data to zero blockage and triple the corrected drag area of a single parachute represented by the open circle gives the required credibility to the cluster data.

Based on the available data, only a tentative discussion of the relationship among the values of K_M for the single parachute and the cluster configurations is possible. It might be argued that the two-parachute cluster illustrated in Fig. 3 presents a shape with a higher aspect ratio than does the single parachute. The concurrent decrease in K_M from 1.85 to 1.35 is qualitatively in agreement with the effect of increasing aspect ratio for rectangular plates reported by Maskell.[3] This reasoning projects that the effective aspect ratio of the three-parachute cluster fell between the other two model configurations. Typically, $C_{p,b}$ increases in magnitude with aspect ratio. Had it been possible to obtain base pressure measurements for the clusters, the connection between $C_{p,b}$ and K_M suggested by Eq. (3) might have provided greater insight into this question.

Conclusions

An extensive wind-tunnel investigation was conducted to gather information on wall-interference effects for parachutes.

A set of nonreefed ribbon parachutes of 7, 15, and 30% geometric porosity was tested in six different wind tunnels covering a range of geometric blockages from 2 to 35%. In addition to single-parachute configurations, clusters of two and three parachutes were studied. The resulting measurements of drag area and canopy base pressure were correlated with the ratio of drag area to tunnel cross section, according to the bluff-body blockage theory of Maskell. An analysis of the experimental data leads to the following conclusions.

1) The Maskell wall-correction equation [i.e., Eq. (2)] was shown to reflect accurately the effective increase in tunnel dynamic pressure for both single parachutes and parachute clusters.

2) For single parachutes, the Maskell blockage factor K_M has a value of 1.85, independent of canopy porosity. Photometric data showed that there was no deformation of the inflated geometry up to the maximum geometric blockage ratio of 0.217.

3) Derived values of K_M for the two- and three-parachute clusters were 1.35 and 1.59, respectively. In the case of the three-parachute cluster, changes in model geometry due to wall constraint were detected at the highest geometric blockage ratio of 0.348; both the inflated diameter and the spacing among member parachutes decreased significantly.

The invariance of the Maskell blockage factor with respect to the porosity of the ribbon parachutes used in this study suggests that the derived values of K_M may be applied to circular and conical canopies in general. And although the reported data are for full-open canopies, the corrections are probably adequate for moderately reefed configurations as well. On the other hand, considering the variation in the blockage factor between a disk and a sphere, tentatively setting $K_M \approx 3.0$ may be more appropriate for very highly reefed, single parachutes. The present data afford no grounds to extrapolate to clusters with more than three parachutes. The data do show that the upper limit on geometric blockage for testing parachutes without significant model deformation due to wall constraint lies between 23 and 35%.

Acknowledgments

This work was supported by the U.S. Department of Energy under Contract DE-AC04-76DP00789. The authors are grateful to Messrs. Brazfield, Peepers, Powers, Smith, Stark, Tate, and Whinery of Sandia Laboratories for their involvement with the models and experiments. We also acknowledge NASA for providing tunnel time at the Ames, Langley, and Lewis Research Centers.

References

[1]Rae, W. H., and Pope, A., *Low-Speed Wind Tunnel Testing,* 2nd ed., Wiley, New York, 1984, Chap. 6.

[2]Hackett, J. E., "Living with Solid-Walled Wind Tunnels," AIAA Paper 82-0583, March 1982.

[3]Maskell, E. C., "A Theory of the Blockage Effects on Bluff Bodies and Stalled Wings in a Closed Wind Tunnel," Royal Aircraft Establishment, United Kingdom, Rept. Aero 2685, Nov. 1963.

[4]Awbi, H. B., "Wind Tunnel Wall Constraint on Two-Dimensional Rectangular-Section Prisms," *Journal of Industrial Aerodynamics,* Vol. 3, No. 4, 1978, pp. 285–306.

[5]Pass, C. Q., "A Wake Blockage Correction Method for Small Subsonic Wind Tunnels," AIAA Paper 87-0294, Jan. 1987.

[6]Awbi, H. B., and Tan, S. H., "Effect of Wind-Tunnel Walls on the Drag of a Sphere," *Journal of Fluids Engineering,* Vol. 103, No. 3, Sept. 1981, pp. 461–465.

[7]Pepper, W. B., and Reed, J. F., "Parametric Study of Parachute Pressure Distribution by Wind Tunnel Testing," *Journal of Aircraft,* Vol. 10, No. 11, Nov. 1976, pp. 895–900.

[8]Holman, J. P., and Gajda, W. J., *Experimental Methods for Engineers,* 4th ed., McGraw-Hill, New York, 1984, Chap. 3.

[9]Holst, H., "Wind Tunnel Wall Interference in Closed, Ventilated and Adaptive Test Sections," *Wind Tunnel Wall Interference Assessment and Correction,* edited by P. A. Newman and R. W. Barnwell, NASA CP-2319, Washington DC, 1984, pp.61–78.

[10]Baca, B. K., "An Experimental Study of the Performance of Clustered Parachutes in a Low-Speed Wind Tunnel," Sandia National Laboratories, Albuquerque, NM, Sandia Rept. SAND85-0813, Dec. 1985.